

## Supported Scorpionate Complexes



## Rapid Synthesis of a Functional Resin-Supported Scorpionate and Its Copper(I, II), Rhodium(I), and Chromium(III) Complexes

Patrick J. Desrochers,<sup>\*[a]</sup> Adam J. Pearce,<sup>[a]</sup> T. Ryan Rogers,<sup>[a]</sup> and Jeremy S. Rodman<sup>[a]</sup>

**Abstract:** Boron-scorpionates are readily prepared by microwave (MW) assisted methods. Such a method is described here, leading to the rapid preparation of a heterogeneous resin-supported scorpionate as its sodium salt, BdPhTpNa [BdPhTp = phenyltris(1-pyrazolyl)borate covalently bound through the phenyl ring to commercial cross-linked polystyrene resin beads]. Formation of a functional heterogeneous scorpionate was confirmed from the subsequent reactions of several metal complexes. This supported ligand system coordinates a variety of transition metal ions including copper(I and II), chromium(III) and rhodium(I). Chromium(III) provided definitive electronic

spectral evidence for supported-TpCr<sup>III</sup> coordination spheres, including reversible ligand-substitution reactions. The copper(I) case exhibited typical scorpionate Cu<sup>I</sup> reactivity including spectroscopically characterized (IR and <sup>31</sup>P NMR) complexes with CO, PPh<sub>3</sub>, and HCCH. Copper(II) provided EPR evidence for heterogeneous scorpionates. The supported rhodium(I) complex was demonstrated to be a recyclable heterogeneous rhodium-scorpionate catalyst. These results all support the conclusion that the immobilized chelate forms coordinatively unsaturated half-sandwich metal complexes (LM<sup>n+</sup>) capable of efficient ligand-substitution reactions or catalytic activity.

## Introduction

Scorpionate chelates represent an established ligand system that has benefitted from 50 years of research, development, and application.<sup>[1,2]</sup> Despite this history, scorpionate contributions to heterogeneous catalysis or combinatorial methods are rare.<sup>[3–5]</sup> This is a significant omission for such a mature ligand class with established reactivity involving the majority of catalytically significant and biologically active metal ions. Historically, covalently tethered metal-free scorpionates have been difficult to prepare. This challenge has limited preparations of tethered boron (usually monoanionic) scorpionates possessing functionally intact N-donor appendages. While some progress has been reported (Figure 1), limitations have included complex reagent sequences requiring long preparation times, leading to few examples of bonafide heterogeneous transition-metal-free scorpionates.

Two persistent challenges must be overcome to accelerate the development of heterogeneous metal scorpionates. First, the efficiency of making heterogeneous scorpionates must be improved. Second, it must be demonstrated that these supported chelates form the kind of functional half-sandwich metal complexes that are best suited for catalytic and bioinorganic applications.<sup>[1,2]</sup>

Microwave (MW) assisted synthesis of scorpionates is a logical solution to the first challenge, because these ligands are generally prepared by the kind of high-temperature thermal

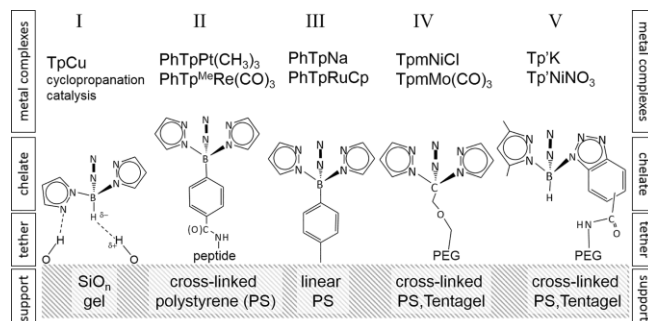


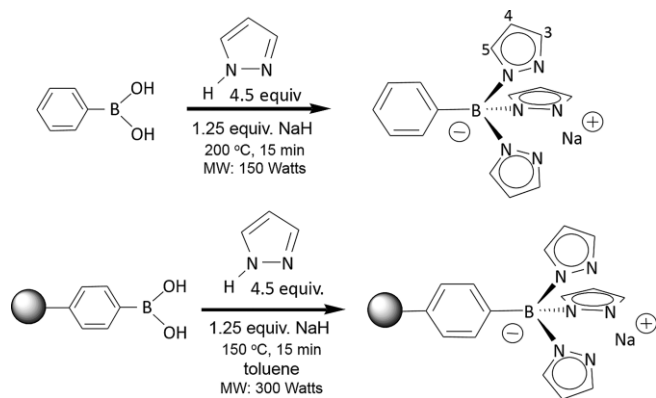
Figure 1. Examples of heterogeneous scorpionates illustrating the variety of supports, tethers, and chelates developed to date. Key metal complexes with these chelates are listed. (I) ref.<sup>[11]</sup>; (II) ref.<sup>[12]</sup>; (III) ref.<sup>[13]</sup>; (IV) ref.<sup>[15]</sup>; (V) ref.<sup>[16]</sup> Third pyrazole rings are shown “on edge” for clarity in these sketches.

routes for which MW methods have demonstrated benefits.<sup>[6]</sup> Rabinovich's group gave the first report in 2006 for the MW preparation of a thioimidazole-based scorpionate.<sup>[7]</sup> A Portuguese patent was granted in 2007 for the microwave-assisted preparation of trispyrazolylmethane (Tpm).<sup>[8]</sup> More recently we reported the preparation of PhTpNa for the first time by microwave methods.<sup>[9]</sup> We were then made aware of independent microwave preparations of KTp and KTp\* by Bitterwolf's group at the University of Idaho.<sup>[10]</sup> The present report builds on this progress and extends MW methods to the preparation of a resin-supported heterogeneous example, BdPhTpNa (Scheme 1).

The second challenge to heterogeneous scorpionate development requires that functional metal scorpionates be prepared. Here, functional refers to half-sandwich metal scorpionates, with several open or at least labile coordination sites on

[a] Department of Chemistry, University of Central Arkansas, Conway, AR 72035, USA  
E-mail: patrickd@uca.edu  
http://uca.edu/

Supporting information and ORCID(s) from the author(s) for this article are available on the WWW under <http://dx.doi.org/10.1002/ejic.201501254>.



Scheme 1.

the metal atom for ligand-substitution reactions and substrate binding. Toward this end supported scorpionates (Figure 1) have employed two different approaches: attach preformed metal scorpionates to solid supports (Figure 1, cases I and II) or build a transition-metal-free scorpionate on a functionalized scaffold, and afterward coordinate the desired metal ion of choice (cases III–V). Cases I and II offer more certain characterization of the homogeneous metal scorpionate before they are anchored.<sup>[11,12]</sup> For Case I the relatively weak hydrogen-bonding attachment made this supported case prone to metal complex leaching with successive uses. Case II is limited to second- and third-row metal ions, where these robust, substitutionally inert metal centers serve as protecting groups for the pyrazole donors during the standard peptide-coupling tether-linking reaction. It would be difficult to remove such metal ions and preserve the integrity of the supported scorpionate for other metal ions. A similar approach of Cases I and II with first-row metal ions was reported by Machado et al. wherein preformed trispyrazolylmethane derivatives of copper(II) and vanadium(IV) (as vandyl) were attached to chlorosulfonylphenyl-functionalized silica nanoparticles.<sup>[5]</sup> These materials were investigated as heterogeneous catalysts in the oxidation of cyclohexane by molecular oxygen.

Cases III–V represent the first reports of covalently anchored half-sandwich complexes where the transition metal ion was added *after* supported ligand synthesis. Jäkle's group reported preparation of the same PhTpNa scorpionate described here on a functionalized linear polystyrene matrix.<sup>[13]</sup> Only a half-sandwich complex of ruthenium(II) was reported with this system. Evidence with copper(II) suggests that this linear polystyrene system was flexible enough to allow formation of (Ligand)<sub>2</sub>Cu sandwich complexes on the resin.<sup>[14]</sup> Cases IV and V represent work from our laboratory,<sup>[15,16]</sup> and both offer the benefits of transition-metal-free chelates capable of coordinating a wide variety of metal ions. Neither gives any evidence of bis-chelate sandwich complex formation, regardless of metal ion employed, due to the dispersion of functional groups across the resin and the rigidity of the cross-linked resin. Case IV incorporates the neutral carbon-based scorpionate, a weaker donor than the anionic boron examples.<sup>[17]</sup> Case V represents the first boron-based heteroscorpionate supported to cross-linked polystyrene,

and functional nickel(II) centers were observed for this chelate system.<sup>[16]</sup>

The metal ions utilized for this present study were chosen for their illustration of some of the same spectroscopic and reactivity behaviors seen for the homogeneous examples. Consequently, rhodium(I) was chosen because of its demonstrated catalytic polymerization of phenylacetylene<sup>[18]</sup> whose deep red-orange color would provide a visual assay of the catalytic effectiveness of the supported metal system. Chromium(III) was chosen, because the general substitutional inertness of this d<sup>3</sup> metal ion provided a robust first-row metal ion platform for confirmatory ligand-substitution reactions.<sup>[19]</sup> Finally copper(I and II) were chosen because of the activity of Tp<sup>R</sup>Cu<sup>I</sup> toward binding small molecules with spectroscopic handles (e.g. CO),<sup>[17]</sup> and copper(II) would be amenable to solid-state EPR spectroscopic measurements.

## Results and Discussion

Resin-supported scorpionates must be stable and capable of readily forming half-sandwich complexes with metals that show useful functionality. Here the dispersed nature of the supported chelates should render them incapable of forming bis-ligand metal sandwich complexes. This is generally true for less flexible, highly cross-linked, polystyrene resin supports; but it remains a limitation of linear polystyrene-supported resins.<sup>[14]</sup> The commercial availability of resin-supported phenylboronic acid facilitates preparation of resin-supported scorpionates by MW methods. In addition, all of the transition metal reactivity described here and observed to date for these systems supports the conclusion that these immobilized ligands form coordinatively unsaturated half-sandwich metal complexes (LM<sup>n+</sup>) with coordination spheres capable of efficient ligand-substitution reactions or catalytic activity.

The phenyltris(pyrazolyl)borate ligand (PhTp<sup>-</sup>) was first reported in 1967 by Trofimenko during the early genesis of the scorpionate ligand class.<sup>[20]</sup> Trofimenko's first conditions were not highly forcing; pyrazole (and no other base) was added in a fourfold molar excess to dichloro(phenyl)borane in toluene, but with no added heat beyond the exothermicity of the reaction itself (up to 55 °C). The PhTp<sup>-</sup> product was never isolated. Instead the toluene reaction mixture was stirred with solutions of various M<sup>2+</sup> cations, and the resulting (PhTp)<sub>2</sub>M complexes were isolated in low yields (17–25 %). A modified synthesis was later reported in 1982 from the reaction of sodium pyrazolide and pyrazole with phenylboronic acid at high temperatures (220 °C, diglyme).<sup>[21]</sup> Again the reported product yield was low (20 %), demonstrating the challenge of forming tetrasubstituted boron centers by this method. This more recent procedure provided impetus for the present work using MW methods (Scheme 1), which are demonstrated by <sup>11</sup>B NMR spectroscopy to quantitatively convert the starting boronic acid into the scorpionate product (Figure S1).

The generality of the method outlined in Scheme 1 suggests that it is applicable to other pyrazoles, especially substituted varieties desirable for tuning the steric and electronic characteristics of the chelate pocket, or other heterocycles (e.g. imidazole

or triazoles). To date, we have only tested pyrazole and 3,5-dimethylpyrazole and the latter only for the homogeneous unsupported case starting from  $\text{PhB}(\text{OH})_2$ . Dimethylpyrazole did not appear to form the desired tridentate chelate (as monitored by  $^{11}\text{B}$  NMR spectroscopy; compare Figure S1). This was the result even at much higher reaction temperatures (170 °C) and prolonged reaction times (30 min). This limitation may result from the steric impediment of the three different 5-position methyl groups (Scheme 1) crowding the phenyl-substituted boron center in this boronic acid synthetic method. We note that  $\text{MTp}^*$  ( $M = \text{Li}, \text{Na}, \text{K}$ ) can be prepared in excellent yields using microwave heating and the conventional scorpionate synthetic route of treating  $\text{KBH}_4$  with molten dimethylpyrazole.<sup>[10]</sup> Future experiments will employ singly substituted (3- or 4-position only) pyrazoles with the expectation that the 3-position substituents will predominately orient away from the boron atom and toward the metal-chelation pocket.

A decided advantage of dispersed resin-supported metal scorpionates is clearly their ability to form coordinatively unsaturated half-sandwich complexes ( $\text{LM}^{\text{n}+}$ ). Such ideals are necessary for metalloprotein model systems and catalytically active metal complexes, two important applications of this ligand system. While second- and third-row metal scorpionates are generally less prone to forming  $\text{L}_2\text{M}$  scorpionates, smaller, more pliable, first-row metal ions are plagued by this problem. This is especially true for the mid- to late-transition series, manganese to zinc.<sup>[1,2]</sup> For the present resin-supported  $\text{BdPhTpNa}$  scorpionate to be useful, it must easily form half-sandwich complexes. Also the metal complexes thus formed must be functional – capable of ligand substitution/metathesis or catalytic activity by exploiting open or labile coordination sites.

All of the metal ions tested to date with the  $\text{BdPhTpNa}$  ligand system exhibit either direct spectroscopic evidence for half-sandwich coordination spheres or else chemical reactivity that supports the same conclusion. This is a significant feature of this resin-supported scorpionate; such coordinatively unsaturated metal centers would not form with  $\text{Tp}^-$ , the least sterically protected scorpionate, free of the resin. If they do form, such complexes are notoriously prone to ligand-exchange disproportionation reactions:  $2\text{Tp}^{\text{R}}\text{MX} \rightarrow (\text{Tp}^{\text{R}})_2\text{M} + \text{MX}_2$ , a prospect eliminated on the current resin support.

### Chromium(III) Reactions

Chromium(III) ion coordinated by  $\text{BdPhTp}$  provided clear ligand metathesis reactivity and spectroscopic evidence for *fac*- $\text{TpCr}^{\text{III}}$  coordination spheres on the resin supports. Chromium(III) was loaded onto the beads using the deep purple anhydrous  $\text{CrCl}_3(\text{THF})_3$  precursor. Typical of chromium(III), the scorpionate coordination reaction took some time, eventually yielding green  $[\text{BdPhTpCrCl}_3]\text{Na}$ . Others have employed granular Zn metal as a reductive catalyst for attaching chromium(III) to *fac*- $\text{N}_3$  chelates;<sup>[22]</sup> future work with this supported ligand system might benefit from this approach. These product beads reversibly bound ammonia gas, evidenced by an obvious change in color of the beads from deep green to light purple (Figure 2). Ammonia could be driven from the beads with moderate heat

(ca. 80 °C warming with a heat gun) causing the purple color to return to the original green of the trichloro complex. Some of these chloro ligands were also irreversibly replaced by cyano ligands by heating green  $[\text{BdPhTpCrCl}_3]\text{Na}$  in a mixture of sodium cyanide and DMF. An IR spectrum of the resulting orange cyano beads revealed a weak but definite  $\nu(\text{CN})$  band at  $2130\text{ cm}^{-1}$  consistent with  $\text{Cr}-\text{CN}$  coordination. Yellow  $[\text{Bu}_4\text{N}][\text{TpCr}(\text{CN})_3]$  has been reported, and structurally characterized, with an observed  $\nu(\text{CN})$  band at  $2114\text{ cm}^{-1}$ .<sup>[23]</sup> This lower frequency for the tricyano system is to be expected due to the backbonding influence of three strong  $\pi$ -acid ligands. A sharp but also weak  $\nu(\text{CN})$  band was observed for  $(\text{Me}_3\text{trcn})\text{Cr}(\text{CN})_3$  at  $2132\text{ cm}^{-1}$ .<sup>[22]</sup>

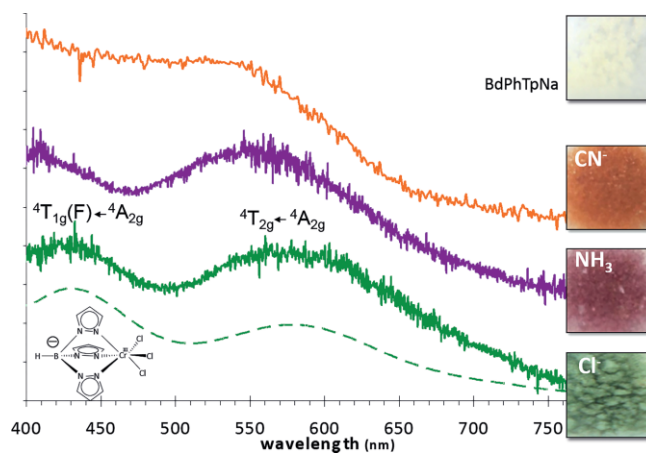


Figure 2. Electronic spectra of  $[\text{BdPhTpCrCl}_3]\text{Na}$ ,  $[\text{BdPhTpCr}(\text{NH}_3)_n\text{Cl}_{3-n}]\text{Na}$ ,  $[\text{BdPhTpCr}(\text{CN})_n\text{Cl}_{3-n}]\text{Na}$  and  $[\text{TpCrCl}_3]\text{Na}$  (dashed). Photographs at right are beads used for each spectrum. A photograph of transition-metal-free  $\text{BdPhTpNa}$  is given at top for comparison.

Electronic spectra collected for each system support describing them all as possessing six coordinate chromium(III) centers (Figure 2). The two visible bands are assigned as the lowest-energy spin-allowed d–d transitions of the  $d^3$  metal ion coordination sphere. A sample of  $[\text{TpCrCl}_3]\text{Na}$  was prepared according to literature methods;<sup>[24]</sup> its electronic spectrum is nearly coincident with the one recorded for  $[\text{BdPhTpCrCl}_3]\text{Na}$ . While the supported complexes show the expected  $\text{Cl}^- < \text{NH}_3 < \text{CN}^-$  ligand-field trend, the amount of  $4\text{T}_{2g} \leftarrow 4\text{A}_{2g}$  energy difference (relative to that of the initial trichloro complex) suggests incomplete substitution of the three chloro ligands of  $[\text{BdPhTpCrCl}_3]\text{Na}$  by ammonia or cyanide. The observed changes in energy when  $\text{Cl}^-$  is replaced by  $\text{NH}_3$  ( $790\text{ cm}^{-1}$ ) or  $\text{Cl}^-$  is replaced by  $\text{CN}^-$  ( $1300\text{ cm}^{-1}$ ) more likely indicate a single ammonia or cyano substitution.<sup>[25]</sup> For comparison, an energy difference of over  $7700\text{ cm}^{-1}$  is observed when three *fac*-chloro ligands are replaced by three *fac*-cyano ligands ( $\text{Me}_3\text{tacnCrX}_3$ ,  $X = \text{Cl}^-$  or  $\text{CN}^-$ ; Table S1).<sup>[22]</sup> Prolonged reaction times and extreme conditions (excess  $\text{NaCN}$  and hot DMF for 3 d) were required to fully convert  $\text{TpCrCl}_3^-$  into  $\text{TpCr}(\text{CN})_3^-$ .<sup>[23]</sup> This substitutional inertness of  $\text{TpCr}^{\text{III}}$  centers is also supported by similarly slow and confirmed single chloro ligand-substitution reaction for  $\text{TpCrCl}_3^-$  with pyridine.<sup>[19b]</sup> Two hours of reflux in acetonitrile/pyridine (17 % v/v pyridine) produced only the single substitution product,  $\text{TpCrCl}_2(\text{py})$ , an analytically pure and structurally

characterized red-violet solid. Interestingly, its visible spectrum (in CH<sub>3</sub>CN:  $\lambda_{\text{max}} = 412 \text{ nm}, 554 \text{ nm}$ ),<sup>[19b]</sup> is essentially the same as was measured here for ammoniated [BdTpCrCl<sub>3</sub>]Na. This strongly suggests that the purple ammoniated solid (Figure 2) can be formulated as [BdPhTpCrCl<sub>2</sub>(NH<sub>3</sub>)](NaCl).

### Copper(I) Reactions

Copper(I) was added to Bd-PhTpNa using the copper(I) salt Cu(NCCH<sub>3</sub>)<sub>4</sub>BF<sub>4</sub> in dry acetonitrile. No color change was discerned in the beads upon coordination of this closed-shell metal ion. This contrasts with the deep green color that develops quickly with BdPhTpNa when methanolic copper(II) halides are added. Similarly, no color change was observed when the copper(I) beads were exposed to carbon monoxide gas under inert conditions. IR analysis of BdPhTpCuCO (KBr pellet) gave a spectrum dominated by resin-supported vibrations, but also showing a strong vibration at 2073 cm<sup>-1</sup> (Figure S2). This vibration is assigned to the Cu<sup>I</sup>CO moiety, and is typical of Tp<sup>R</sup>CuCO reported for homogeneous systems free of resin supports (Table 1). Here CO is a particularly effective ligand for characterizing supported metal coordination spheres. Distinct CO vibrations helped characterize the *fac*-Mo(CO)<sub>3</sub> sphere in resin-supported Bd-TpmMo(CO)<sub>3</sub>,<sup>[16]</sup> and these vibrations were lost with aerial oxidation of the Mo<sup>0</sup> coordination sphere.

Table 1.  $\nu(\text{CO})^{\text{[a]}}$  bands for copper(I) Tp<sup>R</sup>CuCO complexes.

Chelate	$\nu(\text{CO})$ [cm <sup>-1</sup> ]	Ref.
Tp	2083	[26]
Tp <sup>Ms</sup> [b]	2079	[27]
BdPhTp	2073	this work
Tp*	2056	[28]

[a]  $\nu(\text{CO})$ : 2143 cm<sup>-1</sup> for CO(g). [b] Ms = mesityl.

This  $\nu(\text{CO})$  band characterizes BdPhTp<sup>-</sup> as a relatively strong donor ligand toward copper(I), echoing independent electronic spectral results for chromium(III) (Figure S4, Table S1). The frequency measured for BdPhTpCuCO firmly places this system among similar coordination spheres for homogeneous analogues. BdPhTpCuCO reacts with oxygen in air and more rapidly when purged with pure oxygen gas. This oxidation is characterized by a series of visual and spectroscopic changes. The characteristic tan color of the copper(I) beads is replaced by the deep green color of supported copper(II). Carbon monoxide is lost in this change; the original 2073 cm<sup>-1</sup> band diminishes in intensity and is absent in fully oxidized samples.

The resulting green copper(II) beads show an intriguing EPR signature, supporting both the change in oxidation state of copper and the generation of a free radical oxidation byproduct (Figure 3). The copper(II) signal is a typical axial powder pattern with  $g_{\parallel} (2.26) > g_{\perp} (2.07)$ . The  $g_{\perp}$  signal clearly shows a 7-line hyperfine splitting ( $A_{\perp} = 16 \text{ Gauss}$ ) consistent with *fac*-(<sup>14</sup>N)<sub>3</sub>Cu<sup>II</sup> chelation. Seven lines result from coordination of three equivalent nitrogen donor atoms [<sup>14</sup>N, 99.63 %,  $I = 1$ ;  $2(n)I + 1 = 2(3)(1) + 1 = 7$ ]. Collectively, these features support assigning the oxidized copper(II) coordination sphere as possessing a square-pyramidal geometry of the form -TpCu<sup>II</sup>(X,Y).<sup>[29]</sup> At still higher fields a sharp resonance is seen that may be assigned

to a free radical generated from a transient copper(II)-superoxo species.

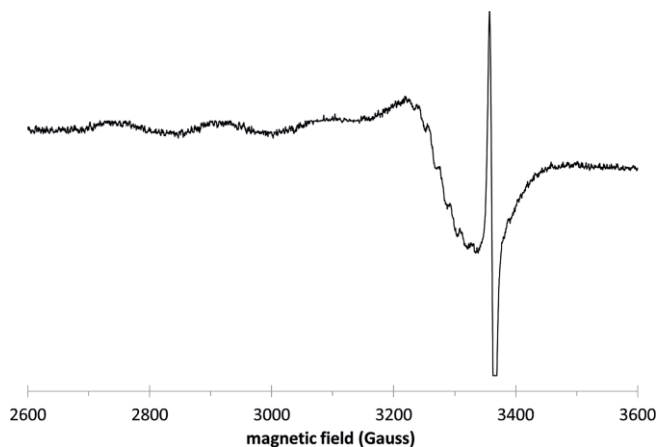


Figure 3. X-band EPR spectrum of BdPhTpCu<sup>II</sup>X following aerial oxidation of BdPhTpCu<sup>I</sup>CO ( $\nu = 9.477 \text{ GHz}$ ). The sharp signal near  $g = 2.014$  represents a radical resulting from the formation of a putative -TpCu<sup>II</sup>(O<sub>2</sub><sup>-</sup>) transient.

Copper scorpionates have been noted for their superoxide dismutase activity.<sup>[30,31]</sup> Extreme ligand steric control is required to prevent the formation of peroxo-bridged dimers of the form Tp<sup>R</sup>Cu<sup>II</sup>( $\mu$ -O<sub>2</sub>)Cu<sup>II</sup>Tp<sup>R</sup>. Accordingly, limited examples of Tp<sup>R</sup>Cu<sup>II</sup>(O<sub>2</sub><sup>-</sup>) are known in which R offers considerable steric protection (R = adamantyl, *tert*-butyl).<sup>[32]</sup> The superoxo groups of such species are still highly reactive. Unfavorable entropic and only mildly favorable enthalpic parameters (Cu-O<sub>2</sub> binding energies = 40–50 kJ/mol) limit isolation of Cu<sup>I</sup>-O<sub>2</sub> complexes to low temperatures.<sup>[33]</sup>

Reaction of these homogeneous systems with dioxygen provides an interesting contrast to the present resin-supported examples. The cross-linked polymer constraints of resin-supported BdPhTp ligand system physically do not allow  $\mu$ -O<sub>2</sub> dimer formation, a decided advantage of resin-supported scorpionates. This means reactive coordinatively unsaturated BdPhTpCu centers result when CO is lost and that dioxygen likely aggressively reacts with the copper center. The mechanism of this oxidation is as yet unknown, but the observed rate of BdPhTpCuCO oxidation is much faster than the rate of BdPhTpCuPPh<sub>3</sub> oxidation (*vide infra*). This likely reflects entropically favorable release of a small CO(g) molecule within the constricted resin matrix vs. the expected more restricted mobility of a larger PPh<sub>3</sub> molecule when lost from the copper(I) center.

Isolable Tp<sup>R</sup>Cu(O<sub>2</sub>) species are deeply colored and diamagnetic, resulting from the spin-coupling of the associated copper(II) and superoxo paramagnets.<sup>[32]</sup> No such deeply colored copper(II)-superoxo complex was observed for the present resin-supported cases. The after effects of a putative Cu(O<sub>2</sub>) transient are evident (Figure 3), therefore some constraint of the resin matrix may be rendering observation of this species impossible for the present system.

### Copper(II)-Acetylene Complex

Dry BdPhTpCu<sup>I</sup> readily binds acetylene when the gas (ca. 1 atm) is introduced to the beads. No outward change is seen in the

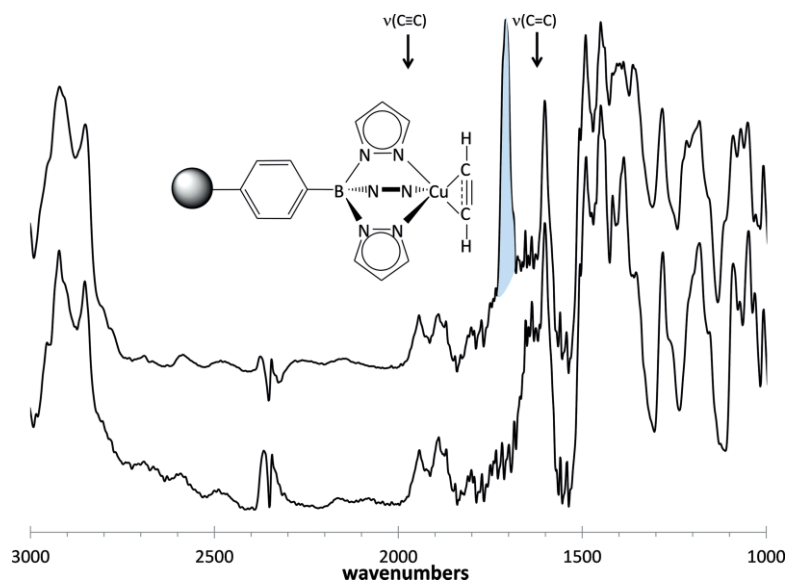


Figure 4. IR spectra of BdPhTpNa (bottom) and BdPhTpCu( $\eta^2$ -HCCH) (top); the band assigned to  $\nu(\text{C}\equiv\text{C})$  of copper-coordinated acetylene is highlighted. Arrows denote gas-phase carbon-carbon stretching frequencies\* for acetylene ( $1974\text{ cm}^{-1}$ ) and for ethylene ( $1623\text{ cm}^{-1}$ ). \*NIST webbook, Raman data.

resin beads when this happens. An IR spectrum (Figure 4) recorded for these beads as a KBr pellet shows a clear band assignable to the carbon-carbon stretch of an  $\eta^2$ -HCCH copper-coordinated acetylene ( $1700\text{ cm}^{-1}$ ), considerably weakened from the free gaseous molecule ( $1974\text{ cm}^{-1}$ ). As with the CO complex, these results indicate the strong electron back-donation of the resin-supported copper scorpionate. The present scorpionate-copper(I)-acetylene complex is consistent with structurally characterized  $\text{Tp}^{\text{Ms}}\text{Cu}(\text{alkynes})$  ( $\text{Ms} = \text{mesityl}$ ),<sup>[34]</sup> and while  $\text{Tp}^{(\text{CF}_3)_2}\text{Ag}(\text{HCCH})$  was also reported, the  $\nu(\text{C}\equiv\text{C})$  value for the coordinated acetylene was not<sup>[35]</sup> (Table 2).

Table 2. Alkyne stretching frequencies in  $\text{Tp}^{\text{R}}\text{M}(\eta^2\text{-alkyne})$  complexes.

$\text{Tp}^{\text{R}}\text{M}(\text{alkyne})$	$\nu(\text{C}\equiv\text{C})$ [ $\text{cm}^{-1}$ ] <sup>[a]</sup>	Ref.
$\text{Tp}^{(\text{CF}_3)_2}\text{Ag}(\text{HCCPh})$	2041 (2110)	[35]
$\text{Tp}^{\text{Ms}}\text{Cu}(\text{HCCPh})$	1923 (2110)	[34]
BdPhTpCu(HCCH)	1700 (1974)	this work

[a] Free alkyne frequency in parentheses.

### Copper(I)-Phosphine

Numerous examples of  $\text{Tp}^{\text{R}}\text{CuPR}_3$  complexes are known, and most are characterized by a diminished sensitivity to oxygen vs. their comparative CO complexes. This prompted an experiment in which copper(I)-loaded beads were treated with triphenylphosphine in diethyl ether to see if the coordinated phosphine could be identified using  $^{31}\text{P}$  NMR spectroscopy and if similar oxidative stability could be achieved for BdPhTpCu<sup>I</sup>. We note that the coordination of triphenylphosphine to BdPhTpCu<sup>I</sup> appears to be slow, and very slow in donor solvents like acetonitrile. After 3 h of reaction time, the beads were washed with diethyl ether, transferred to an NMR tube to which was then added  $[\text{D}_3]\text{acetonitrile}$ . These beads sink in acetonitrile, but the action of spinning during the NMR measurement lifts the beads from the bottom of the tube into the spinning vortex allowing a meaningful spectrum to be recorded (Figure 5). The recorded

spectrum exhibited a sharp resonance assigned to some  $\text{O}=\text{PPh}_3$  at  $\delta = 26\text{ ppm}$  and a broad resonance at  $\delta = -2.8\text{ ppm}$  assigned to the resin-supported  $\text{Cu}-\text{PPh}_3$  group. This downfield-shift value relative to that of free phosphine is in the range of other  $\text{Tp}^{\text{R}}\text{Cu}(\text{phosphine})$  complexes (Table 3).

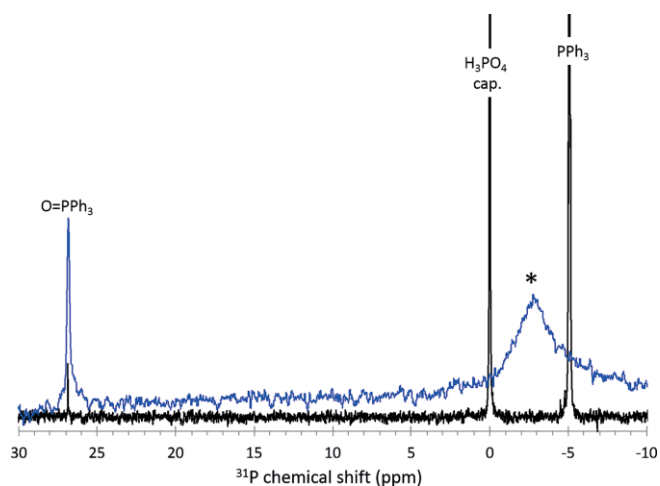


Figure 5.  $^{31}\text{P}$  NMR spectra of BdPhTpCuPPh<sub>3</sub> (in  $\text{CD}_3\text{CN}$ ; blue) and of PPh<sub>3</sub> in  $\text{CH}_3\text{CN}$  with a  $0.5\text{ M H}_3\text{PO}_4(\text{aq})$  capillary added (black). The broad resonance assigned to resin-supported  $\text{TpCuPPh}_3$  is marked with an asterisk.

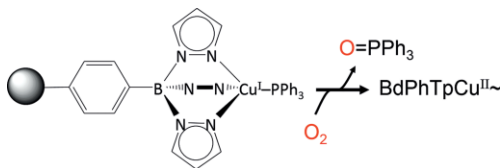
Table 3.  $^{31}\text{P}$  NMR chemical shift values for various  $\text{Tp}^{\text{R}}\text{Cu}^{\text{I}}-\text{PR}_3$  complexes.

<i>fac</i> -Chelate	$\text{PR}_3$	$\delta(^{31}\text{P})$ [ppm] <sup>[a]</sup>	Solvent	Ref.
Tp	PPh <sub>3</sub>	-6.12	$\text{CDCl}_3$	[36]
BdPhTp	PPh <sub>3</sub>	-2.8	$\text{CD}_3\text{CN}$	this work
Tp*	PPh <sub>3</sub>	-4.99	$\text{CDCl}_3$	[36]
Tp <sup>Me</sup>	$\text{PPh}_2(\text{PhCO}_2\text{H})$	-1.6	$\text{CDCl}_3$	[31]
pZTp <sup>Me</sup>	$\text{PPh}_2(\text{PhCO}_2\text{H})$	-0.2	$\text{CDCl}_3$	[31]
HB(Btz) <sub>3</sub> <sup>[b]</sup>	$\text{PPh}_2(\text{PhCO}_2\text{H})$	5.6	$(\text{CD}_3)_2\text{CO}$	[31]

[a] Values of free ligand:  $\text{PPh}_2(\text{PhCO}_2\text{H})$ :  $\delta = -4.8\text{ ppm}$  ( $\text{CDCl}_3$ );<sup>[31]</sup> PPh<sub>3</sub>:  $\delta = -5.1\text{ ppm}$  ( $\text{CD}_3\text{CN}$ ); PPh<sub>3</sub>:  $\delta = -6.0\text{ ppm}$  ( $\text{CDCl}_3$ ).<sup>[37]</sup> [b] HB(Btz)<sub>3</sub> = hydrotris(1-benzotriazolyl)borate.

No discernible color change was seen when  $\text{PPh}_3$  coordinates with  $\text{BdPhTpCu}^{\text{I}}$ . Coordination of  $\text{PPh}_3$  to  $\text{BdPhTpCu}^{\text{I}}$  was evident in the complete lack of oxidation seen with the dry beads exposed to air for over a week. The same exposure for  $\text{BdPhTpCu}^{\text{I}}$  (absent CO or  $\text{PPh}_3$ ) results in the beads developing their characteristic green copper(II) color in open air in less than 20 min.

A sample of  $\text{BdPhTpCuPPh}_3$  in chloroform was exposed to oxygen. Within minutes the beads developed a green color. This behavior with triphenylphosphine is reminiscent of oxo-transfer reactions observed for homogeneous copper(I) scorpionates;<sup>[38]</sup> however, here an environmentally much more friendly oxidant was employed ( $\text{O}_2$ ) vs. the industrial oxidant, Oxone. A  $^{31}\text{P}$  NMR spectrum recorded for the supernatant in contact with the beads showed a strong signal at  $\delta = 32$  ppm assignable<sup>[39]</sup> to  $\text{O=PPh}_3$  formed as a result of the reaction of the  $\text{Cu-PPh}_3$  moiety with  $\text{O}_2$  (Scheme 2). The formation of phosphine oxide was evidently directed by the copper(I) precursor, because triphenylphosphine alone under the same conditions does not form the oxide in its absence.



Scheme 2.

Copper(I) scorpionates have demonstrated the ability to act as radical initiators by abstracting halogen atoms from halocarbons.<sup>[40]</sup> Light amber  $\text{BdPhTpCu}$  reacts immediately with  $\text{CX}_4$  ( $\text{X} = \text{Cl}$  or  $\text{Br}$ ) giving the beads a distinctive red-brown coloration (Figure 6 and Figure S3) typical of  $\text{Tp}^{\text{R}}\text{CuX}$  coordination spheres that have been isolated as maroon or red-brown solids with sterically much more demanding scorpionates ( $\text{R} = \text{tert-butyl}$ ,  $\text{isopropyl}$ ).<sup>[29,40,41]</sup> This is reminiscent of Kharasch reactions catalyzed by  $\text{Tp}^{\text{R}}\text{Cu}^{\text{I}}$  centers (e.g., the addition of  $\text{Cl-CCl}_3$  across the  $\text{C=C}$  bond of styrene). A diffuse-reflectance elec-

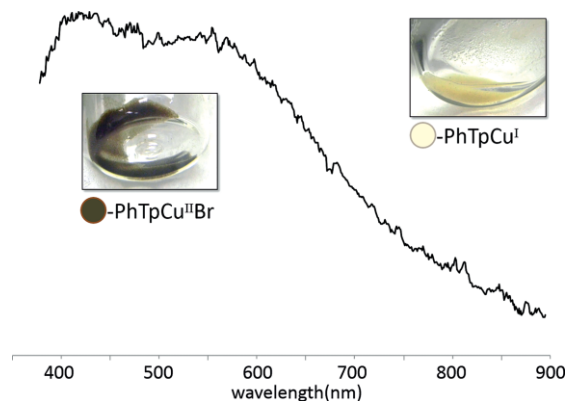


Figure 6. Inset pictures:  $\text{BdPhTpCu}^{\text{I}}$  (right) in diethyl ether,  $\text{BdPhTpCu}^{\text{II}}\text{Br}$  (left) resulting from addition of  $\text{CBr}_4$  in diethyl ether to  $\text{BdPhTpCu}$ . Electronic spectrum (by diffuse reflectance) of washed and dried  $\text{BdPhTpCu}^{\text{II}}\text{Br}$  ( $\lambda_{\text{max}} = 425, 550$  nm).

tronic spectrum recorded for the maroon bromo form had a pair of broad absorbances near 425 and 550 nm.

### Rhodium(I) Reactions

Rhodium(I) is a second-row metal ion with established catalytic activity involving scorpionate chelates. It is readily coordinated to  $\text{BdPhTpNa}$  using  $[\text{RhCl}(\text{cod})]_2$  in warm THF, imparting a distinct yellow color to the resulting product beads,  $\text{BdPhTpRh}(\text{cod})$ , which appear to be stable toward air and moisture. The primary goal of these rhodium tests was to prove that the heterogeneous rhodium(I) complex could function as a recyclable catalyst, with no drop off in catalytic activity with successive uses. The reaction chosen was the polymerization of phenylacetylene (PhAc), a reaction for which  $\text{Tp}^{\text{R}}\text{Rh}(\text{cod})$  has proven catalytic efficacy and one in which the brightly colored polymer product would afford a visual assay of the extent of the polymerization.

The polymerization reaction was conducted five successive times with the same sample of  $\text{BdPhTpRh}(\text{cod})$  using the experimental conditions described by Katayama et al.<sup>[18]</sup> At the end of each run, the  $\text{BdPhTpRh}(\text{cod})$  beads were isolated from the reaction mixture by introducing diethyl ether, lowering the mixture density, causing the beads to sink (Figure 7). The supernatant product mixture was assayed for extent of reaction by electronic spectroscopy, monitoring the absorbance near 450 nm. The beads were thoroughly washed with diethyl ether in the Schlenk tube, minimizing loss of the catalyst beads from one run to the next. Each time the beads were dried of residual diethyl ether under a nitrogen stream.

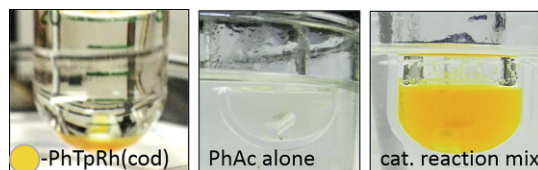


Figure 7.  $\text{BdPhTpRh}(\text{cod})$  in  $\text{CH}_2\text{Cl}_2$ /diethyl ether (left), PhAc alone in  $\text{CH}_2\text{Cl}_2$  after warming to  $40^\circ\text{C}$  (center). Reaction mixture containing  $\text{BdPhTpRh}(\text{cod})$  + PhAc in  $\text{CH}_2\text{Cl}_2$  after 24 h at  $40^\circ\text{C}$ . Note  $\text{BdPhTpRh}(\text{cod})$  floats in this mixture.

Successive runs with the same catalyst beads confirmed that  $\text{BdPhTpRh}(\text{cod})$  functions as a recyclable heterogeneous catalyst. The extent of reaction in each case was small (2–5 %, also verified by  $^1\text{H}$  NMR spectroscopy), despite the consistent color change due to polyphenylacetylene,  $(\text{PhAc})_n$ , formation in the mixture. Two different control experiments confirmed that the  $\text{BdPhTpRh}(\text{cod})$  was indeed catalytically forming  $(\text{PhAc})_n$  (Figure 7). One mixture included phenylacetylene in solvent but no  $\text{BdPhTpRh}(\text{cod})$ . The other control mixture used the same  $\text{BdPhTpRh}(\text{cod})$  beads in solvent but without added phenylacetylene. Both control mixtures remained colorless, confirming that  $(\text{PhAc})_n$  did not form in the absence of  $\text{BdPhTpRh}(\text{cod})$  and that the yellow coloration observed in all repetitive catalyzed mixtures did not result from leaching of the yellow rhodium complex from the resin.

The low-percent conversion could imply that the matrix constraints of the present cross-linked PS support render the nor-

mally very active  $\text{Tp}^{\text{R}}\text{Rh}(\text{cod})$  less active for formation of  $(\text{PhAc})_n$ . Clearly limitations of the present resin support for this particular reaction are evident, motivating continued development of new resin adaptations.<sup>[42]</sup> On the current support, it is reasonable to assume the rate of polymer growth slows considerably for the catalytically active rhodium center that must accept additional PhAc monomer while contending with  $-\text{Tp}$  and  $\text{cod}$  chelates and the growing polymer chain in a crowded resin environment. This conclusion is consistent with the fact that the dry resin matrix is highly permeable to small gaseous molecules ( $\text{CO}$ ,  $\text{O}_2$ , and  $\text{HCCH}$  with  $\text{BdPhTpCu}^{\text{I}}$ ), but slower to react when bulky solvated reagents are involved ( $\text{PPh}_3$  toward  $\text{BdPhTpCu}^{\text{I}}$  and PhAc toward the active rhodium catalyst). Work involving this and other supported rhodium catalysts will help define the optimum catalytic role for this heterogeneous rhodium scorpionate catalyst system.

## Conclusions

Because boron-based scorpionates are generally prepared by thermal routes, their synthesis is greatly accelerated using microwave heating methods. The efficiency of this approach led to the generation of the simplest scorpionate,  $\text{Tp}^-$ , as its phenyl-substituted derivative obtained from phenylboronic acid. Progress in these reactions was monitored using  $^{11}\text{B}$  NMR spectroscopy. This success motivated the subsequent preparation of the resin-supported analogue,  $\text{Bd-PhTp}^-$ , as its sodium salt. Microwave preparation of this supported chelate is a significant achievement both in terms of the simplicity of the reagents used and efficiency of the method developed to prepare it. The route is limited in its ability to functionalize all of the resin-supported  $-\text{PhB}(\text{OH})_2$  groups to the corresponding scorpionate. Given the ease of conversion of resin-free  $\text{PhB}(\text{OH})_2$  to the corresponding chelate, the limitation seen with the present resin matrix, while commercially accessible, appears to be less than ideal for forming supported scorpionates. Identification of an optimum matrix for rapid MW-assisted preparation of supported scorpionates is ongoing including work with starch-based supports.

Importantly, the present  $\text{BdPhTp}$  scorpionate demonstrated the kind of reactivity expected for this *fac*-chelate ligand class with transition metal ions,  $\text{Cr}^{\text{III}}$ ,  $\text{Cu}^{\text{I}}$ , and  $\text{Rh}^{\text{I}}$ . All of the reactivity seen with these metal ions can be characterized as resulting from unsaturated  $\text{TpM}^{\text{n}}$  coordination spheres. Resin-dispersed chelates operate without the explicit steric protection necessary to prevent sandwich complexes ( $\text{TpMTp}$ ), thermodynamic dead-ends seen with unsupported ligands, a decided advantage over homogeneous scorpionates.

Spectroscopic and reactivity evidence observed for all of these metal ions mirror their homogeneous  $\text{TpM}$  counterparts. Electronic spectroscopic measurements confirmed the formation of  $[\text{BdPhTpCrCl}_3]\text{Na}$  as well as the sluggish ligand-substitution reactivity predicted for this  $d^3$  chromium(III) center. The reversibility of these ligand substitutions could only occur with and provides firm evidence for coordinatively unsaturated  $\text{TpCr}^{\text{III}}$  centers in these complexes. Reactions involving copper(I) confirmed the permeability of the resin matrix to small gaseous

molecules and gave products analogous to homogeneous  $\text{Tp}^{\text{R}}\text{CuCO}$  and  $\text{Tp}^{\text{R}}\text{Cu}(\eta^2\text{HCCH})$  examples. Additional reactivity of the copper(I) case with halocarbons and triphenylphosphine are all consistent with resin-supported  $\text{TpCu}$ , as well as the axial EPR spectra recorded for resulting copper(II) products. Here a heterogeneous rhodium(I) scorpionate is described for the first time, and is demonstrated to possess recyclable catalytic activity toward phenylacetylene polymerization. Collectively, these results demonstrate sufficient breadth of reactivity to motivate the future preparation of variants of this supported ligand system as well as their extension to an even wider array of metal ions. This should expand the reach of the mature scorpionate ligand class to transition-metal-based heterogeneous catalysis, combinatorial methods, small-molecule sensors, and functional/supported metalloprotein mimics.

## Experimental Section

**General:** All microwave-assisted reactions were carried out in a computer-controlled CEM Discover MW Synthesizer. Resin-supported phenylboronic acid beads [abbrev.  $\text{BdPhB}(\text{OH})_2$ ] were obtained from Alfa Aesar. These resin beads are primarily cross-linked polystyrene with an average boron functional-group density of 3 mmol/g of resin. It should be noted that this resin matrix is more robust than TantaGel PEG resin on which our earlier work was supported.<sup>[16]</sup> Reaction mixtures involving the present resin could be vigorously stirred with little visible effect on the integrity of the solid support (unlike TantaGel PEG resin). Acetonitrile was dried by refluxing and distillation from  $\text{CaH}_2$ , THF and  $\text{Et}_2\text{O}$  from potassium/benzophenone, and DMF by storing over 4 Å molecular sieves all under dry nitrogen for 24 h.

**Spectroscopy:** IR spectra were recorded using a Thermoline spectrometer for samples as KBr pellets. NMR spectra were recorded using a JEOL ECX-300 MHz spectrometer. NMR spectra on resin samples required long acquisition times, typically 20 h or more. X-band EPR spectra were recorded for solid resin samples in quartz tubes using a Resonance Instruments Model 8400 spectrometer coupled with an EIP Model 545A microwave frequency counter. Solid-state electronic spectra were recorded for resin-bead samples between glass microscope slides using a Varian Cary 50 spectrometer and a video Barrelineo diffuse-reflectance attachment (Harrick Scientific).

**Microwave Synthesis of  $\text{PhTpNa}$ :** A small (10 mL), thick-walled microwave reaction tube was charged with phenylboronic acid (500 mg, 4.10 mmol, Acros Organics), pyrazole (1.25 g, 22.3 mmol, Acros Organics) and sodium hydride (126 mg, 5.25 mmol, Sigma). The tube was sealed with a PTFE septum, and the mixture was placed under nitrogen through a needle fitting. The mixture was heated in the microwave synthesizer at 200 °C (150 mW maximum power setting, allowing 5 min ramp time to reach the temperature) for 10 min. In practice, the maximum power setting was rarely seen once the programmed hold temperature was reached. In general the power consumption during the hold period drops precipitously to little more than 5–10 % of the maximum setting. The resulting residue was assayed by drawing a sample adhering to a glass stirring rod from the MW tube and dissolving this sample from the rod in  $[\text{D}_6]\text{DMSO}$ .  $^{11}\text{B}$  NMR spectra recorded for this sample confirmed the conversion into the target ligand (Figure S1).

**Microwave Synthesis of  $\text{BdPhTpNa}$ :** A typical preparation involved mixing  $\text{BdPhB}(\text{OH})_2$  [500 mg, 1.5 mmol of  $-\text{PhB}(\text{OH})_2$  functional group], pyrazole (1.27 g, 23 mmol) and sodium hydride (40 mg,

1.7 mmol) in a 30 mL thick-walled MW reaction tube with a Teflon-coated stir bar. The tube was fitted with a silicone-PTFE MW septum, and the mixture was placed under dry nitrogen. While stirring, degassed toluene (4 mL) was added by cannula to this mixture. The mixture was treated using the program of a 10 min ramp time to 150 °C (max. power 300 mW) where the temperature was held for 15 min. Subsequently, the mixture was cooled to room temperature using compressed gas in about 5 min. The resulting resin beads were washed six times with toluene (3 mL) followed by six additional washings with diethyl ether and dried under a nitrogen stream. During each washing the beads were stirred in contact with the solvent for 3–5 min. The final dry beads were noticeably more amber in color relative to their precursor starting material. An  $^{11}\text{B}$  NMR spectrum recorded for these beads suspended in  $[\text{D}_6]\text{DMSO}$  revealed a broad resonance ( $w_{1/2} \approx 1600$  Hz) centered at  $\delta = -3$  ppm.

**Metal Loading:** This was determined for several different samples of  $\text{BdPhTpCuCl}$  beads (vide infra). Weighed (50–100 mg) samples of dry copper-loaded beads were digested in 10 M  $\text{HCl}(\text{aq})$  for several hours, liberating the copper(II) as  $\text{CuCl}_4^{2-}$ . Released copper was quantified spectrophotometrically by visible-light absorption of this complex ion in each sample. The copper loading ranged between 5 and 10 % of the available functional-group density [reported as 3 mmol  $-\text{PhB}(\text{OH})_2/\text{g}$  of initial resin]. Variations in ligand-bead preparations, including crushing the beads and extended soaking in the toluene solvent prior to MW heating, did not improve the metal loading beyond what is reported. While free boronic acids readily form scorpionates using the method described, this specific resin matrix may be limited in its ability to support scorpionate groups.

**Preparation of  $[\text{BdPhTpCrCl}_3]\text{Na}$ :**  $\text{BdPhTpNa}$  was treated with anhydrous  $\text{CrCl}_3(\text{THF})_3$  prepared in an MBraun glove box with dry THF and anhydrous  $\text{CrCl}_3$ . Addition of the deep purple solution of  $\text{CrCl}_3(\text{THF})_3$  to the beads caused them to darken. After stirring at room temperature for ca. 10 min, the beads assumed a deep green color with a noticeable decrease in color of the supernatant liquid. The beads were washed 4 times with dry THF (3 mL), 2 times with dry diethyl ether, and then dried under a stream of dry nitrogen.

**Reversible Reaction of  $[\text{BdPhTpCrCl}_3]$  with  $\text{NH}_3(\text{g})$ :** Deep green  $[\text{BdPhTpCrCl}_3]\text{Na}$  solid was placed in a flow-through glass tube fitted with a glass-wool plug such that gases could pass over the stationary solid without the solid being pushed through the tube. Through a two-way stopcock, the system was first flushed with nitrogen, and then the gas flow (10 mL/min, 1 atm) was switched to anhydrous ammonia. As the ammonia passed over the solid, a definite color change was observed for the beads from green to light purple. The ammonia purge was continued until the sample had a uniform purple color (ca. 10 min). The sample was then flushed with nitrogen to remove extraneous ammonia gas, and an electronic spectrum of the beads was recorded by diffuse reflectance. Subsequently, the same purple beads in the glass tube were placed back under a nitrogen stream while being warmed externally with a heat gun (80–90 °C). The original green color of the  $[\text{BdPhTpCrCl}_3]\text{Na}$  beads re-emerged within 1 min of this treatment.

**Reaction of  $[\text{BdPhTpCrCl}_3]$  with  $\text{NaCN}$ :** A sample of green  $[\text{BdPhTpCrCl}_3]\text{Na}$  (40 mg) was placed in a 25 mL Schlenk tube and charged with sodium cyanide (17 mg) and dry DMF (1 mL). The mixture was heated to 80 °C and stirred for 60 min. Over time the green color of the beads changed to a light orange. After 70 min under these conditions, the mixture was cooled, and the product beads were washed 4 times with DMF (2 mL). The beads were subsequently washed 5 times with diethyl ether (5 mL) and dried under a nitrogen stream. An electronic spectrum of the beads was re-

corded by diffuse reflectance. An IR spectrum was recorded for the orange beads (as a KBr pellet;  $\nu(\text{CN})$ : 2130  $\text{cm}^{-1}$ ).

**Preparation of  $\text{BdPhTpRh}(\text{cod})$ :** A 25 mL Schlenk flask was charged with  $\text{BdPhTpNa}$  (50 mg) and  $[\text{RhCl}(\text{cod})]_2$  dimer (5.1 mg, Strem) and placed under dry nitrogen. Dry degassed THF (3 mL) was added to this mixture, which was stirred under nitrogen at 40 °C for 16 h. Subsequently, the beads were repeatedly washed 5 times with dry THF (2 mL). Each washing involved stirring the beads in contact with the solvent for 5–10 min. Finally, the now bright yellow beads were washed 2 times with diethyl ether (2 mL) and then dried under a nitrogen stream.

**Polymerization of Phenylacetylene:** A typical reaction used  $\text{BdTPRRh}(\text{cod})$  (19 mg) in a Schlenk tube, followed by dichloromethane (2 mL) as a solvent, and phenylacetylene (100  $\mu\text{L}$ ) as the monomer for the polymerization under nitrogen. The reaction mixture was warmed in an oil bath at 40 °C and stirred for 1 d. The supernatant was diluted with diethyl ether to a total volume of 20 mL, and an electronic spectrum was recorded with a background of  $\text{Et}_2\text{O}/\text{CH}_2\text{Cl}_2$  (18:1, v/v). The absorbance at 425 nm was recorded and compared for successive runs. Before each subsequent repetition, the beads were washed several times with  $\text{CH}_2\text{Cl}_2$  (5 mL, soaking with stirring for 5–10 min) followed by several washings with  $\text{Et}_2\text{O}$  and drying under a nitrogen stream.

**Preparation of  $\text{BdPhTpCu}^I$ :** Under dry nitrogen, a sample of  $\text{BdPhTpNa}$  (185 mg) was stirred in contact with a solution prepared from  $\text{Cu}(\text{NCCCH}_3)_4\text{BF}_4$  (175 mg) dissolved in dry  $\text{CH}_3\text{CN}$  (5 mL). Immediately upon contacting the resin beads, the originally clear and colorless  $\text{Cu}^I$  solution yielded a fine white precipitate (presumably solid  $\text{NaBF}_4$ ). The mixture was stirred for an additional 20 min. Subsequently, the opaque supernatant was decanted, and the remaining resin beads were washed repeatedly with dry  $\text{CH}_3\text{CN}$  until the washings were no longer cloudy (5–7 times, 5 mL, each with stirring). The beads were washed 2 times with diethyl ether (2 mL) and dried under a nitrogen stream. The beads in this form are stable indefinitely under an inert gas.

**Addition of CO and HCCH to  $\text{BdPhTpCu}^I$ :** The  $\text{BdPhTpCu}^I$  product beads were exposed to a stream of CO (ca. 1 atm, 10 mL/min) while in a Schlenk tube, originally under dry nitrogen. Subsequently, a sample of these CO-exposed beads was formed into a KBr pellet and the FTIR spectrum recorded. A clear  $\nu(\text{CO})$  band was visible at 2073  $\text{cm}^{-1}$ . The same exposure method with acetylene and a new sample of  $\text{BdPhTpCu}^I$  beads yielded an FTIR spectrum with a strong  $\nu(\text{C}\equiv\text{C})$  band at 1700  $\text{cm}^{-1}$ .

**Preparation of  $\text{BdPhTpCuPPh}_3$ :** Copper(I) was loaded onto a sample of  $\text{BdPhTpNa}$  (200 mg) as described above; however, following the washing regimen described, the beads were allowed to remain wet with diethyl ether. To this mixture was added a solution of triphenylphosphine (216 mg) in dry diethyl ether (3 mL). The mixture was stirred for 2 h. Subsequently, the supernatant was removed, and the product beads were washed with diethyl ether. The wet beads were suspended with  $\text{CD}_3\text{CN}$  in an NMR tube, and a  $^{31}\text{P}$  NMR spectrum was recorded:  $\delta = -2.8$  ppm (br.) and  $\delta = 26.8$  ppm due to some  $\text{Ph}_3\text{P}=\text{O}$  formed in the sample.

**Supporting Information** (see footnote on the first page of this article):  $^{11}\text{B}$  NMR spectrum of  $\text{PhB}(\text{OH})_2$  and the  $\text{PhTpNa}$  ligand product mixture; IR spectrum of  $\text{BdPhTpCuCO}$ ; comparative electronic spectra of resin- $\text{TpmCrCl}_3$  and  $[\text{BdPhTpCrCl}_3]\text{Na}$  and a table summarizing ligand-field transitions for these and other  $\text{fac-}N_3\text{CrCl}_3$  species.

## Acknowledgments

The majority of this work was funded by the National Science Foundation (CHE-0717213). T. R. R. is grateful to the UCA STEM grant for summer-stipend support. The UCA College of Natural Sciences and Mathematics provided funding for the purchase of the microwave synthesizer. We are grateful to Prof. R. Tarkka and P. Cook (UCA Chemistry) for their early work on microwave synthesis of scorpionates that provided impetus for this work. We thank Prof. L. Yang (UCA Chemistry) for supplying the copper(II) salt starting materials used in this work. We also thank Prof. J. Telser for helpful comments on the copper EPR work.

**Keywords:** N ligands · Scorpionates · Immobilization · Microwave chemistry

- [1] a) S. Trofimenko, *Polyhedron* **2004**, *23*, 197–203; b) S. Trofimenko, *Scorpionates: The Coordination Chemistry of Polypyrazoloborate Ligands*, Imperial College Press, London, U. K., **1999**.
- [2] C. Pettinari, *Scorpionates II: Chelating Borate Ligands*, Imperial College Press, London, U. K., **2008**.
- [3] N. E. Leadbeater, M. Marco, *Chem. Rev.* **2002**, *102*, 3217–3274. This review details progress in polymer-supported mainstream metal chelates including phosphines, salens, porphyrins, and metallocenes. The omission of scorpionates from this review is significant. Progress during the recent intervening decade will change this.
- [4] a) M. P. de Almeida, L. M. D. R. S. Martins, S. A. C. Carabineiro, T. Lauterbach, F. Rominger, A. S. K. Hashmi, A. J. L. Pombeiro, J. L. Figueiredo, *Catal. Sci. Technol.* **2013**, *3*, 3056–3069; b) L. M. D. R. S. Martins, M. P. de Almeida, S. A. C. Carabineiro, J. L. Figueiredo, A. J. L. Pombeiro, *Chem-CatChem* **2013**, *5*, 3847–3856. A June 2014 SciFinder search on heterogeneous catalysis/combinatorial methods turned up hundreds of hits involving phosphines, porphyrins, bipyridines, salens, and metallocenes.
- [5] K. Machado, S. Mukhopadhyay, G. S. Mishra, *J. Mol. Catal. A* **2015**, *400*, 139–146.
- [6] C. O. Kappe, D. Dallinger, S. S. Murphree, *Practical Microwave Synthesis for Organic Chemists: Strategies, Instruments and Protocols*, Wiley-VCH, Weinheim, **2009**.
- [7] L. S. Maffett, "Microwave-Assisted Syntheses of Scorpionate-Type Ligands", MS thesis, University of North Carolina, Charlotte, **2007**. The preparation of hydrotris(2-thioimidazolyl)borate is described.
- [8] A. J. Pombeiro, L. de Oliveira, L. M. D. R. S. Martins, E. C. B. A. Alegria, Portuguese Pat. No. 103681 A 20070629, **2007**. Tpm = tris(1-pyrazolyl)methane; Tp<sup>−</sup> = hydrotris(1-pyrazolyl)borate.
- [9] PhTpNa = phenyltris(1-pyrazolyl)borate, sodium salt. Philip R. Cook, Tristan W. Phillips, Richard M. Tarkka, Patrick J. Desrochers, 241st ACS National Meeting, Anaheim, CA, March **2011**, INOR-333.
- [10] D. Rabinovich, T. Bitterwolf, private communications.
- [11] M. M. Diaz-Requejo, T. R. Belderrain, M. C. Nicasio, P. J. Pérez, *Organometallics* **2000**, *19*, 285–289.
- [12] M. C. Kuchta, A. Gross, A. Pinto, N. Meltzler-Nolte, *Inorg. Chem.* **2007**, *46*, 9400–9404.
- [13] Y. Qin, C. Cui, F. Jäkle, *Macromolecules* **2008**, *41*, 2972–2974.
- [14] P. O. Shipman, C. Cui, P. Lupinska, R. A. Lalancette, J. B. Sheridan, F. Jäkle, *ACS Macro Lett.* **2013**, *2*, 1056–1060. Copper(II) addition produced light blue resin-Tp<sub>2</sub>Cu sandwich complexes, leading to aggregation of the linear polystyrene support.
- [15] P. J. Desrochers, A. L. Corken, R. M. Tarkka, B. M. Besel, E. E. Mangum, T. N. Linz, *Inorg. Chem.* **2009**, *48*, 3535–3541.
- [16] P. J. Desrochers, B. M. Besel, A. L. Corken, J. R. Evanov, A. L. Hamilton, D. L. Nutt, R. M. Tarkka, *Inorg. Chem.* **2011**, *50*, 1931–1941. Resin-Tp<sup>−</sup>K represents the supported heteroscorpionate hydrobis(3,5-dimethylpyrazolyl)(1-benzotriazolyl)borate.
- [17] K. Fujisawa, T. Ono, Y. Ishikawa, N. Amir, Y. Miyashita, K.-i. Okamoto, N. Lehnert, *Inorg. Chem.* **2006**, *45*, 1698.
- [18] H. Katayama, K. Yamamura, Y. Miyaki, F. Ozawa, *Organometallics* **1997**, *16*, 4497–4500.
- [19] a) A. F. R. Kilpatrick, S. V. Kulangara, M. G. Cushion, R. Duchateau, P. Mountford, *Dalton Trans.* **2010**, *39*, 3653–3664; b) J. M. Abrams, R. Fagiani, C. J. L. Lock, *Inorg. Chim. Acta* **1985**, *106*, 69–74.
- [20] S. Trofimenko, *J. Am. Chem. Soc.* **1967**, *89*, 6288–6294.
- [21] D. L. White, J. W. Faller, *J. Am. Chem. Soc.* **1982**, *104*, 1548–1552.
- [22] M. P. Shores, P. A. Berseth, J. R. Long, *Inorg. Synth.* **2004**, *34*, 149–155. Me<sub>3</sub>tacn = 1,4,7-trimethyl-1,4,7-triazacyclononane.
- [23] T. D. Harris, J. R. Long, *Chem. Commun.* **2007**, 1360–1362.
- [24] R. Rojas, M. Valderrama, G. Wu, *Inorg. Chem. Commun.* **2004**, *7*, 1295–1297.
- [25] A. B. P. Lever, *Inorganic Electronic Spectroscopy*, Elsevier, New York, **1968**, p. 275. Comparative chromium(III) <sup>4</sup>T<sub>2g</sub> ← <sup>4</sup>A<sub>2g</sub> transition energies: CrCl<sub>6</sub><sup>3−</sup> 13180 cm<sup>−1</sup>, Cr(NH<sub>3</sub>)<sub>6</sub><sup>3+</sup> 21550 cm<sup>−1</sup>, Cr(CN)<sub>6</sub><sup>3−</sup> 26700 cm<sup>−1</sup>.
- [26] M. I. Bruce, A. P. P. Ostazewski, *J. Chem. Soc., Dalton Trans.* **1973**, 2433–2436.
- [27] J. L. Schneider, S. M. Carrier, C. E. Ruggiero, V. G. Young Jr., W. B. Tolman, *J. Am. Chem. Soc.* **1998**, *120*, 11408–11418.
- [28] C. Mealli, C. S. Arcus, J. L. Wilkinson, T. J. Marks, J. A. Ibers, *J. Am. Chem. Soc.* **1976**, *98*, 711–718.
- [29] N. Kitajima, K. Fujisawa, Y. Morooka, *J. Am. Chem. Soc.* **1990**, *112*, 3210–3212.
- [30] C. Santini, M. Pellei, G. G. Lobbia, D. Fedeli, G. Falcioni, *J. Inorg. Biochem.* **2003**, *94*, 348–354.
- [31] C. P. Santini, M. G. G. Lobbia, S. Alidori, M. Berrettini, D. Fedelli, *Inorg. Chim. Acta* **2004**, *357*, 3549–3555.
- [32] P. Chen, D. E. Root, C. Campochario, K. Fujisawa, E. I. Solomon, *J. Am. Chem. Soc.* **2003**, *125*, 466–474.
- [33] E. A. Lewis, W. B. Tolman, *Chem. Rev.* **2004**, *104*, 1047–1076.
- [34] C. Martin, M. Sierra, E. Alvarez, T. R. Belderrain, P. J. Pérez, *Dalton Trans.* **2012**, *41*, 5319–5325.
- [35] H. V. R. Dias, Z. Wang, W. Jin, *Inorg. Chem.* **1997**, *36*, 6205–6215.
- [36] G. G. Lobbia, C. Pettinari, F. Marchetti, B. Bovio, P. Cecchi, *Polyhedron* **1996**, *15*, 881–890.
- [37] C. Ohrenberg, L. M. Liable-Sands, A. L. Rheingold, C. G. Riordan, *Inorg. Chem.* **2001**, *40*, 4276–4283.
- [38] M. M. Diaz-Requejo, T. R. Belderrain, P. J. Pérez, *Chem. Commun.* **2000**, 1853–1854. Oxone is the industrial name for the peroxomonosulfate ion.
- [39] V. V. Grushin, *Chem. Rev.* **2004**, *104*, 1629–1662.
- [40] J. M. Muñoz-Molina, A. Caballero, M. M. Díaz-Requejo, S. Trofimenko, T. R. Belderrain, P. J. Pérez, *Inorg. Chem.* **2007**, *46*, 7725–7730.
- [41] K. Yoon, G. Parkin, *Polyhedron* **1995**, *14*, 811–821.
- [42] J. Lu, P. H. Toy, *Chem. Rev.* **2009**, *109*, 815–838.

Received: October 30, 2015

Published Online: April 26, 2016